International Journal of Robotics and Control Systems
Vol. 3, No. 1, 2023, pp. 107-119
ISSN 2775-2658
http://pubs2.ascee.org/index.php/ijrcs

Controlling Pulse-Like Self-Sustained Oscillators Using Analog Circuits and Microcontrollers

Ulrich Simo Domguia [a,1,*], Raoul Thepi Siewe [b, 2]

[a] Department of Mechanical Engineering, University of Buea, P.O. Box 63, Buea, Cameroon
[b] Laboratory on Modelling and Simulation in Engineering, Biomimetics and Prototypes, and TWAS Research Unit, University of Yaounde I, Box 812, Yaounde, Cameroon
[1] simo_ulrich@yahoo.fr; [2] thepiraoul@yahoo.com
* Corresponding Author

ARTICLE INFO

Article history
Received September 21, 2022
Revised November 09, 2022
Accepted February 02, 2023

Keywords
Pulse-like oscillators;
Brusselator oscillators;
Microcontrollers;
analog circuits;
Control;
Synchronization

ABSTRACT

Using simulation from analog electronic circuits and from a microcontroller, this paper considers the control or synchronization of pulse-like self-sustained oscillators described by the equations derived from the chemical system known as Brusselator. The attention is focused on the effect of proportional control when the Brusselator is subjected to disturbances such as pulse-like oscillations and square signals. The analog electronic circuits simulation is based on Multisim, while the microcontroller simulation uses mikroC software and PIC 18F4550. In order to determine the intervals for which the synchronization is effective, the equations of the Brusselator are solved numerically using the fourth-order Runge-Kutta method. As software used for conducting numerical simulations, FORTRAN 95 version PLATO is used for numerical simulation and MATLAB for plotting curves using the data generated from FORTRAN simulations. It has been shown that the control is effective for some values of the proportional control parameter. A good qualitative and quantitative agreement is found from the results of the numerical simulation and those obtained from the analog electronic circuits as well as those delivered by the microcontroller. Since the oscillations delivered by the heart are pulsed oscillations, this study gives an idea of how to control the heart frequency of an individual whose heart is subject to certain disturbances related to stress or illness, to name just a few examples.

1. Introduction

For many years, coupled nonlinear oscillators have been a source of growing interest in different research fields, ranging from physics, chemistry, and engineering to biology and social sciences [1–5]. Between these oscillators, two main classes are to be distinguished: the forced and the self-sustained oscillators, among which are pulse-like self-sustained oscillators. These pulse-like self-sustained oscillators are of interest in chemistry and biological science. They give some idea on the functioning of several systems such as the respiratory system, digestive system, nervous system, etc. [6], delay systems [7], biological systems [8], and chemical systems [9], to name just a few examples. Because of the special localized shape of the oscillations, they can be used in man-made devices such as actuation tasks in industries. For biomimetic applications, they can indicate some ideas on how the heart membrane responds to the action of some neuronal activities. They can also give some hints for the fabrication of artificial ventricles or in the nowadays research activities for artificial heart design [10].

The system used in this paper is a chemo-inspired self-sustained oscillator named Brusselator oscillator, which is a system known in the context of self-catalytic chemical reactions. It was first analyzed by Prigogine and Lefever in 1968 [11]. They proposed a two variables model with periodic oscillations that are asymptotically stable. This two variables model was first referred to as the "trimolecular model." Subsequently, he substituted that of Brusselator in reference to the town of Brussels, where it was discovered. This oscillator permits to study of self-catalyzed chemical reactions when stability is verified. In the 1970s, nonlinear oscillations and bifurcations were discovered first by modeling and then by experiments for the autocatalytic Brusselators and the Belousov-Zhabotinsky (BZ) chemical reactions [12, 13]. The autocatalytic chemical reaction phenomenon plays a vital role in the breakdown of the stability of the thermodynamical branch.

When self-sustained oscillators are subjected to the effect of perturbations, they suffer distortions and phase shifts [14]. These disturbances can have consequences in the context of applications when there is a need for precision, as the phase shift leads to the change of times at which prescribed actions are needed. When this happens, and for the sake of applications, it is of interest to put in place a control scheme that will rapidly mitigate the effects of the perturbation. Several control strategies exist: moving from using proportional-derivative-integral control to more sophisticated ones such as adaptive controls [15-17].

The goal of this work is to conduct a control of the action of perturbation on the pule-like signals generated by the Brusselator oscillator using both an analog electronic circuit and a microcontroller. The case of microcontroller simulation is of special interest as it uses embedded technology, which is today more reliable than analog electronic circuits [18-26]. The paper is organized as follows. Section 2 deals with the control in the model with analog electronic components. In Section 3, the control based on microcontroller technology is undertaken. Section 4 presents the conclusion.

2. Control in the Analog Model

2.1. Description of the Electronic Model of the Brusselator Oscillator

The set of equations describing the Brusselator oscillator is

$$\begin{cases} \dfrac{dx_s}{d\tau} = a - x_s^2 y_s - (b+1)x_s \\ \dfrac{dy_s}{d\tau} = -bx_s - x_s^2 y_s \end{cases} \tag{1}$$

where x_s and y_s are the concentrations of the interacting chemical species. a and b are externally-controlled concentrations.

This set of equations can be transformed into equations deriving from an electronic circuit. Such an analog electronic model of the Brusselator oscillator is presented in Fig. 1. It consists of integrator-summing circuits with operational amplifiers A1 and A2 (all of the LF356 series) whose polarization can take values between -15V and 15V. The other components are voltage multipliers M1 and M2 of the AD633JN series. These multipliers operate with a symmetrical power supply of values between -18V and 18V. Their average current consumption is 4 mA. C_1 and C_2 are capacitors of ceramic series and components referenced by R_k ($1 \leq k \leq 5$) denote resistors.

2.2. Modeling Equations of the Brusselator Oscillator

Let us put v_S, V_1, V_2 and v_{Sy}, the voltages at the output of the first integrator (A1), the output of the first multiplier (M1), the output of the second multiplier (M2) and the output of the second integrator (A2), respectively. The output voltage of the multiplier used in this manuscript is obtained from the following equation as

$$\mathrm{W} = \frac{(x_1 - x_2)(y_1 - y_2)}{V_{ref}} + z_1 \tag{2}$$

where x_1, x_2, y_1, y_2 are the input voltages of the multiplier; z_1 is an additional input generally connected to the ground; V_{ref} is scaling voltage whose value is 10 V. Thus, V_1 and V_2 are expressed as follows:

$$V_1 = \frac{v_S^2}{10},\ \mathrm{V}_2 = \frac{V_1 v_S}{10} = \frac{v_S^2 v_{Sy}}{100} \tag{3}$$

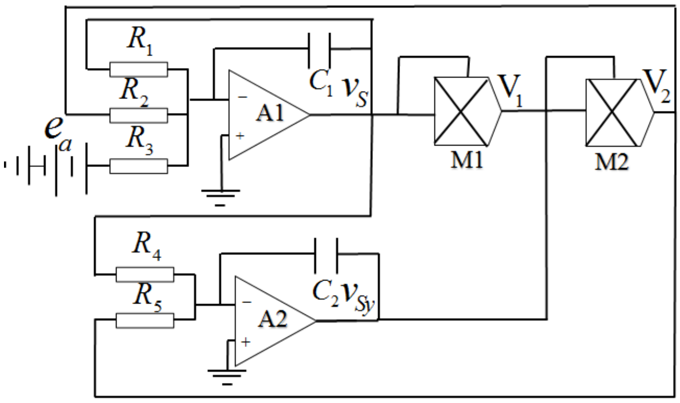

Fig. 1. The equivalent electrical circuit of the Brusselator oscillator

Let us also consider I_1, I_2, I_3, I_4, I_5, I_{11} and I_{22} the current intensities in the resistance of the resistors R_1, R_2, R_3, R_4, R_5, the inverting input of the first integrator and the inverting input of the second integrator. Their expressions are written as follows:

$$I_1 = \frac{v_S}{R_1}\ ; \mathrm{I}_2 = \frac{V_2}{R_2}\ ; \mathrm{I}_3 = -\frac{e_a}{R_3}\ ; \mathrm{I}_4 = \frac{v_{Sy}}{R_4}\ ; \mathrm{I}_5 = \frac{V_2}{R_5}\ ; \mathrm{I}_{11} = -C_1\frac{dv_S}{dt_b}\ ; \mathrm{I}_{22} = -C_2\frac{dv_{Sy}}{dt_b} \tag{4}$$

Using the nodes law, one obtains

$$\begin{cases} I_{11} = I_1 + I_2 + I_3 \\ I_{22} = I_4 + I_5 \end{cases} \tag{5}$$

The equations of the electrical part according to Kirchhoff's laws are thus given as follows:

$$\begin{cases} \dfrac{dv_S}{dt_b} = -\dfrac{v_S}{R_1C_1} - \dfrac{v_S^2 v_{Sy}}{100R_2C_1} + \dfrac{e_a}{R_3C_1} \\ \dfrac{dv_{Sy}}{dt_b} = -\dfrac{v_S}{R_4C_2} - \dfrac{v_S^2 v_{Sy}}{100R_5C_2} \end{cases} \tag{6}$$

The following dimensionless variables are used:

$$\tau = \omega_1 t_b\ ;\ v_S = u_0 x_s\ ;\ v_{Sy} = u_0 y_s\ ;\ e_a = u_0 E_a \tag{7}$$

where $\omega_1 = 104$ Hz is the reference frequency adopted for a good choice of electronic components and $u_0 = 1\,V$ is the reference voltage.

Thus, the dimensionless equations of the Brusselator are given as follows:

$$\begin{cases} \dfrac{dx_s}{d\tau} = a - x_s^2 y_s - (b+1)x_s \\ \dfrac{dy_s}{d\tau} = -bx_s - x_s^2 y_s \end{cases} \tag{8}$$

with the following dimensionless coefficients:

$$a = \frac{E_a}{R_3 C_1 \omega_1} \ ; \ \frac{u_0^2}{100 R_2 C_1 \omega_1} = 1 \ ; \ b + 1 = \frac{1}{R_1 C_1 \omega_1} \ ; \ b = \frac{1}{R_4 C_2 \omega_1} \ ; \frac{u_0^2}{100 R_5 C_2 \omega_1} = 1 \quad (8)$$

Equation (8) is similar to Equation (1).

2.3. Proportional control of a Brusselator Oscillator Subjected to a Square Disturbance

When the Brusselator oscillator is subjected to a perturbation, there appears a distortion of its output and phase shift. Controlling the distortion and the phase shift means here to force the perturbed state of the oscillator to come back to its referenced or prescribed state. This can be understood as synchronizing the actual or perturbed Brusselator oscillator to the state of a reference Brusselator. So, we consider in this Section two Brusselator electronic oscillators, one of which is not subjected to any disturbance and the other one subjected to a square-type perturbation. Both oscillators are coupled in a master-slave configuration, as shown in Fig. 2. v_S represents the reference oscillator and v_x the perturbed oscillator has to follow the dynamics of the reference oscillator. The controller coefficient here is given by the relation $k_p = \frac{R_{SX}}{R_C}$. By introducing this last expression, the system shown in Fig. 2 can be described by a set of four differential equations as

$$\begin{cases} \dfrac{dx_s}{d\tau} = a - x_s{}^2 y_s - (b+1) x_s \\ \dfrac{dy_s}{d\tau} = -b x_s - x_s{}^2 y_s \\ \dfrac{dx}{d\tau} = a - x^2 y - (b+1)x + u + p(t) \\ \dfrac{dy}{d\tau} = -bx - x^2 y \end{cases} \quad (9)$$

where the master system is described by the parameters x_s and y_s, and the system slave or actual system by the parameters x and y. $p(t)$ is the square disturbance voltage whose expression is given below:

$$p(t) = \frac{sin[w(t - t_i)]}{|sin[w(t - t_i)]|} \quad (10)$$

where w is the frequency of the square disturbance and t_i the time when the perturbation is localized.

The u is the controller responsible for mitigating the effects of the disturbance in order to bring the system back to its normal motion or to the state of the master system. Here, we first consider u a linear proportional controller given as follows:

$$u = k_p e = k_p (x - x_s) \quad (11)$$

The values of the capacitors and resistances used in Fig. 2 are given in Table 1.

Table 1. Values of capacitors and resistances used in the overall electronic circuit of Fig. 2.

Resistances (Ω), capacitors (nF)	Master oscillator (j=1)	Slave oscillator (j=2)
R_{j1}	Variable (10000)	Variable (10000)
R_{j2}	100	100
R_{j3}	Variable (250000)	Variable (250000)
R_{j4}	Variable (10000)	Variable (10000)
R_{j5}	100	100
R_0	180000	180000
R	40000	4000
C_{j1}	10	10
C_{j2}	10	10

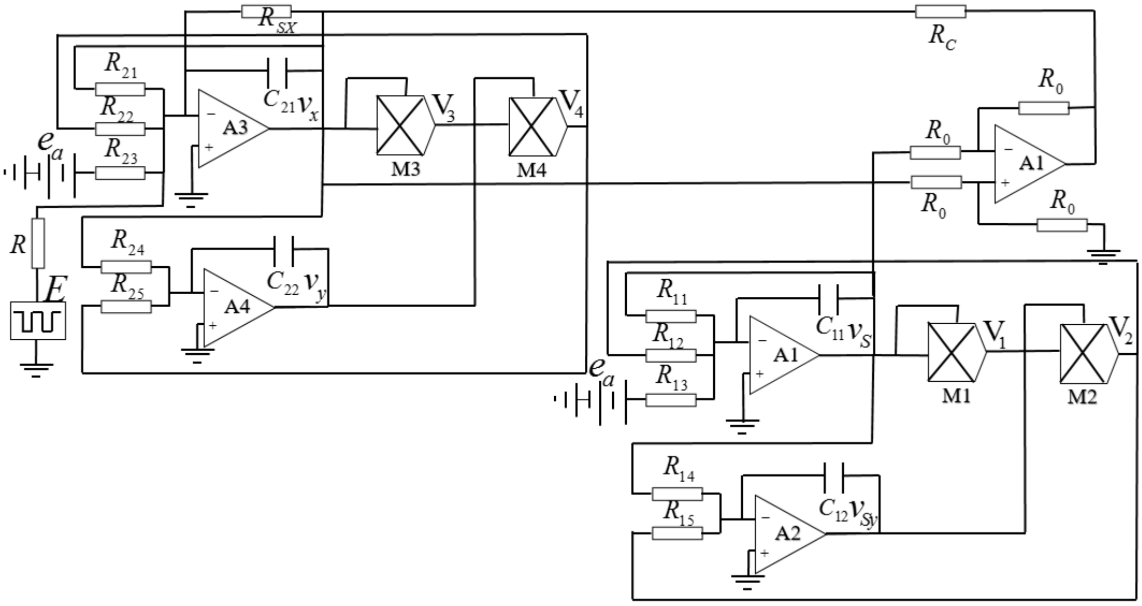

Fig. 2. The equivalent electrical circuit of two Brusselator oscillators coupled in the master-slave scheme.

2.3.1. State of the Oscillators in the Absence of Control

Setting $k_p = 0$ (no control), Fig. 3 shows in blue the Brusselator in its normal or reference state and in red in its disturbed state, both the numerical simulation (Fig. 3 (a)) and analog simulation results (Fig. 3 (b)). We used the fourth-order Runge-Kutta algorithm for the numerical simulations of Equation (9) and the Multisim software to simulate the electronic circuits.

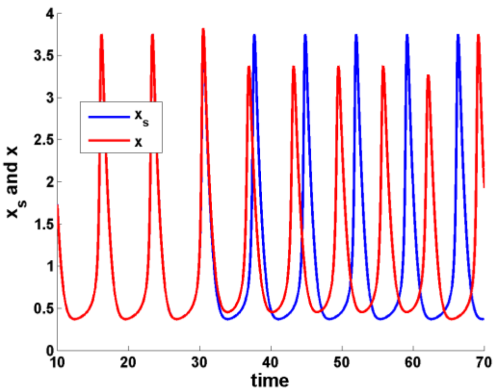

(a)

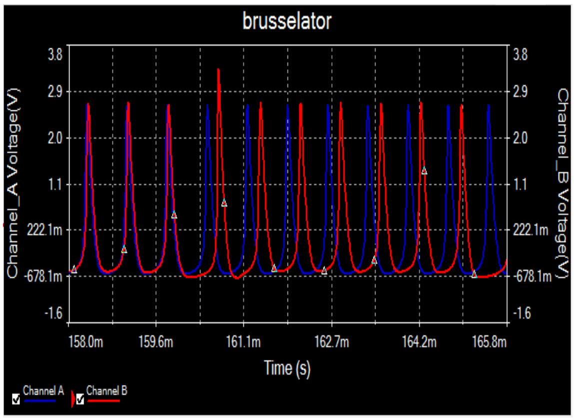

(b)

Fig. 3. The behavior of the Brusselator oscillator was obtained from the numerical simulation (a) and from the analog electronic simulation (b) with the parameters $a = 1$ and $b = 3$.

In Fig. 3 (a), the perturbation is localized at time t = 30. It is observed at this time that the oscillator leaves its normal trajectory and moves to a new trajectory with a different amplitude. After the perturbation ($t \in [35,65]$), there is a shift of the oscillations, with this time a decrease of the amplitude of the disturbed signal with respect to the normal state. When $t \geq 65$, the disturbed signal returns to its normal amplitude, but a phase shift is observed between the normal state and the perturbed state. Fig. 3 (b) shows that at t = 160.30 ms, the perturbation is effective, and the amplitude increases in the perturbed signal. After the perturbation, the amplitude returns to the normal state, but again, there is a phase shift between the normal state and the perturbed state. The next section is thus to find the appropriate values of the control coefficient that will quickly mitigate the effects of the perturbation by limiting the amplitude variation and canceling the phase shift.

2.3.2. Effectiveness of the control

We find in this section the values of k_p for which the control is effective. This is carried out in the numerical simulation using the normalized average synchronization error, which is defined as

$$\sigma = \sqrt{\frac{\langle (x(t) - x_s(t))^2 \rangle}{\langle x(t)^2 \rangle} + \frac{\langle (y(t) - y_s(t))^2 \rangle}{\langle y(t)^2 \rangle}} \tag{12}$$

where $\langle . \rangle$ denotes the time average. The normalized average synchronization error is a quantitative indicator measuring the time-averaged proximity between the reference state x_s and the actual or perturbed state x. Fig. 4 presents this error versus the control parameter k_p.

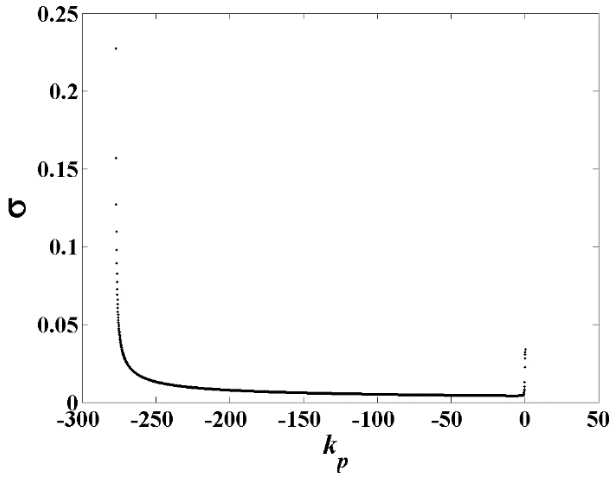

Fig. 4. Normalized average synchronization error σ versus the control coefficient k_p.

Synchronization or control is effective when σ is close to zero. Fig. 4 shows that the control is effective when $k_p < 0$ and good for small values of k_p. The control degrades as k_p increases (in the negative direction) until k_p = -276.95. Thus, the interval of k_p for which the control is effective is $k_p \in [-277; 0]$.

Now considering the analog electronic model and the Multisim simulation, Fig. 5 presents two examples where the control is effective: in blue, the reference state x_s and in red the actual state x of the Brusselator oscillator as delivered by the electronic device. Varying the value of R_{SX} or R_C, one arrives at the conclusion that the electronic model leads to effective control for $k_p \in [-278; 0]$; an interval that is similar to the one obtained from the numerical simulation.

3. Control in the Microcontroller Model

3.1. Control of a Brusselator Oscillator Subjected to a Pulse-like Shape Perturbation

Due to the difficulty of implementing the square signal as a disturbance in the mikroC simulation software, we use in this Section a perturbation having a pulse-like shape and mathematically defined by

$$p(t) = \frac{s_1}{1 + \frac{[s(t-t_i)]^2}{2}} \tag{13}$$

where s_1 and s are, respectively, the amplitude and width of the pulse-like perturbation while t_i is the time corresponding to the highest amplitude of the perturbation. We thus consider the system of Equation (9) with the perturbation given by Equation (13).

Vol. 3, No. 1, 2023, pp. 107-119

<table>
<tr><th>Values of k_p</th><th colspan="2">Temporal trace</th></tr>
<tr><td>-2</td><td>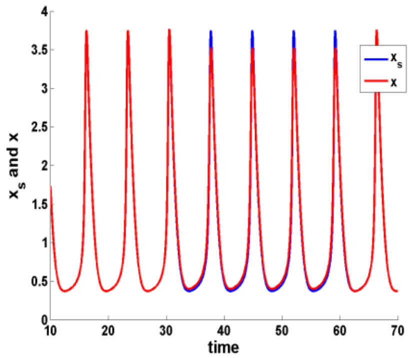
</td><td>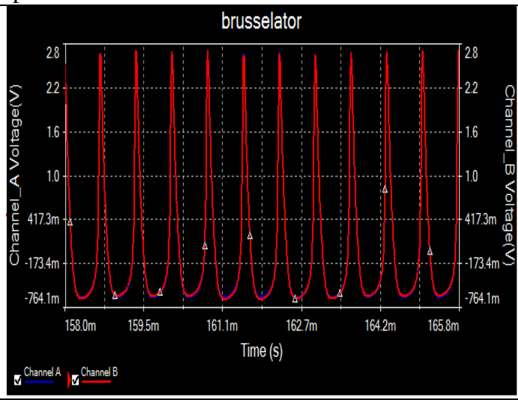
</td></tr>
<tr><td>-250</td><td>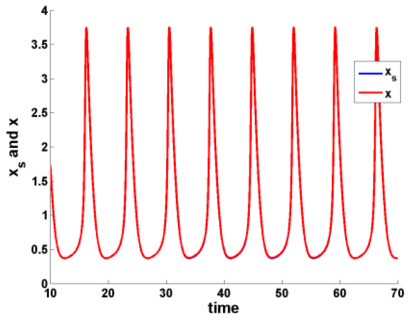
</td><td>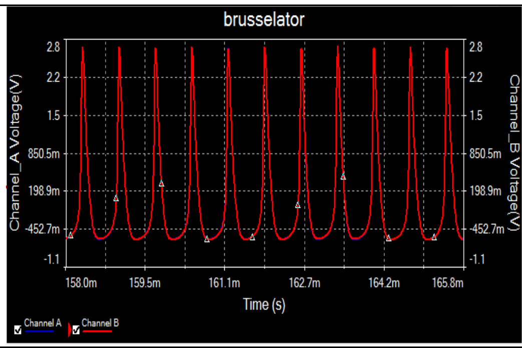
</td></tr>
</table>

Fig. 5. Control situation for many values of k_p.

3.2. Construction of the Digital Simulator on Microcontroller and Simulation on Proteus Software

We use in this section the normalized equations of the Brusselator given by Equations (9) with the parameters $a = 1$ and $b = 3$. With these parameter values, the Brusselator oscillator delivers pulse-like outputs. In order to implement the oscillator equations into the microprocessor, we discretize the Brusselator equations using the Euler method. The equations resulting from this transformation are given as

$$\begin{cases} x_s(k+1) = x_s(k) + ts[a - x_s(k)^2 y_s(k) - (b+1)x_s(k)] \\ y_s(k+1) = y_s(k) + ts[-bx_s(k) - x_s(k)^2 y_s(k)] \\ x(k+1) = x(k) + ts\left[\, a - x(k)^2 y(k) - (b+1)x(k) + k_p(x(k) - x_s(k)) + p(t)\right] \\ y(k+1) = y(k) + ts[-bx(k) - x^2(k)y(k)] \end{cases} \tag{14}$$

where $ts = 0.01$ is the sampling time.

Fig. 6 shows the electronic circuit used to implement the Brusselator oscillator. A microcontroller PIC 18F4550 from Microchip® was used. The ports B and D of the microcontroller were coupled to the R-2R ladder resistors network, which acts as a DAC (digital to analog converter). The microcontroller and the R-2R DAC were selected because they are inexpensive and simple to configure. The outputs of the DAC were taken from the resistors labeled R16 and R32, and they correspond to the outputs $x_s(t)$ and $x(t)$ of the Brusselator oscillators. Notice that the outputs of the systems are in continuous time after the ladder resistors network. But it is also possible to take the output in the discrete-time mode.

To test the implementation, the code shown in Fig. 7 was developed using the mikroC compiler. The result of the $x_s(k)$ and $x(k)$ variables were routed to Ports B and D of the microcontroller and converted into analog voltage by the R-2R DAC. Thus, the outputs result $x_s(t)$ and $x(t)$. The instructions TRISB and TRISD are used to configure Ports B and D as digital outputs. After computing the equations, the results were sent to Ports B and D. The output voltages were digitalized through an oscilloscope (Tektronics, series 2008).

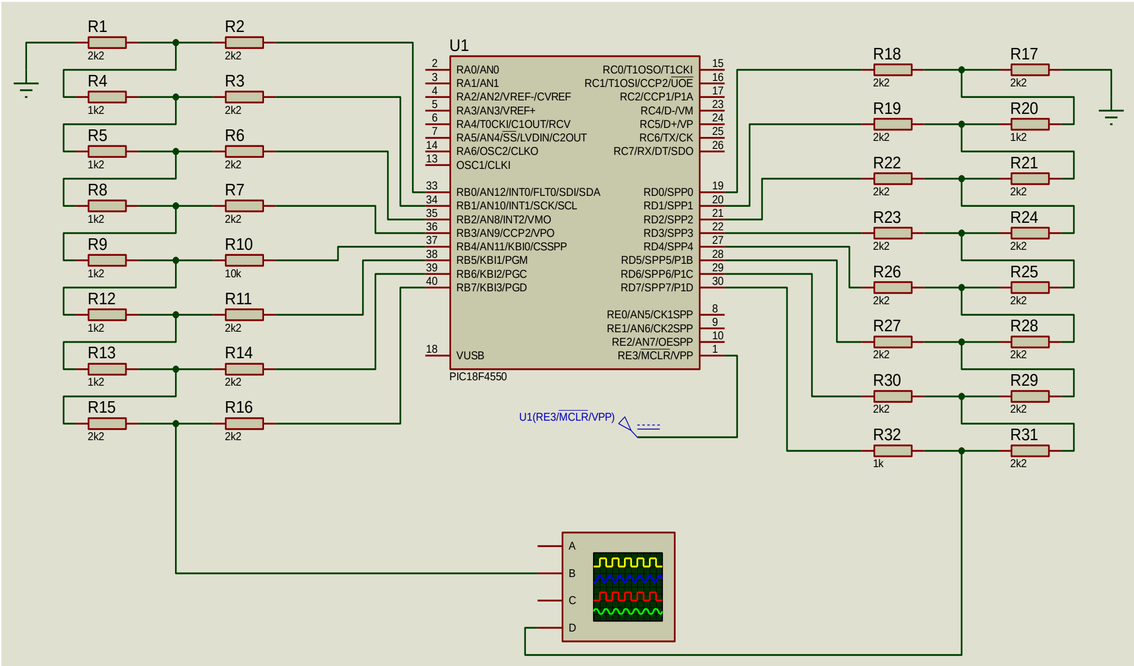

Fig. 6. The electronic circuit is used to implement the pulse-like self-sustained oscillators in the microcontroller.

3.3. Response in the Absence of Control

To ascertain the comparison to be made between the results from the numerical simulation and those obtained from the simulation through the microcontroller, we plot in Fig. 8 the shape of the perturbation given by the numerical plot and the one generated in the microcontroller.

By taking into account the above perturbation, we obtain Fig. 9 representing in blue the reference state and in red the perturbed state. In Fig. 9 (a) and Fig. 9 (b), the perturbation is localized at time t = 285. As in the preceding section, the perturbation creates a distortion, leading to an increase in the amplitude of oscillations at this time and to a slow steep drop thereafter before returning to the reference amplitude. After the perturbation, there is a phase shift of the oscillations between the reference state and the actual state.

3.4. Effectiveness of the Control Using a Microcontroller

We find in this section the values domain of k_p for which the control is successful in order to make a comparison between numerical and microcontroller simulation. Fig. 10 presents the normalized synchronization error versus the control parameter. From the numerical simulation, one also finds that the control is efficient for $k_p \in [-278; 0]$.

The same analysis has been undertaken using the microcontroller simulation. Fig. 11 displays some examples of cases leading to the control. As mentioned above, the reference state is in blue, while the actual state is in red. From the microcontroller simulation, the interval of k_p for which the control is effective is $k_p \in [-201; 0]$. In comparison to the interval obtained from the numerical simulation, one notices a large difference. This can be explained by the fact the simulation through the microcontroller uses the Euler scheme, which can be a source of lack of precision.

In comparison to the results of the previous research, remind that Thepi et al. in 2017 presented a study based on Microcontroller Control/Synchronization of the Dynamics of Van der Pol Oscillators Submitted to Disturbances [14]. They used three control methods, among which the proportional control method, for the synchronization of their oscillators. They used the synchronization time to determine the intervals of the proportional coefficient for which control was effective. They implemented these values in the microcontroller and found good agreement with the numerical results. Regarding our work, we use chemo-inspired oscillators and apply the proportional control method for the synchronization of the oscillators. We use the normalized synchronization error to determine the intervals of the coefficient for which the control is effective. We implement these values in the analog model and the one obtained by microcontroller programming and find a good agreement with the numerical results.

```
#pragma config PLLDIV = 5
#pragma config FOSC = HSPLL_HS, FCMEN = OFF, IESO = OFF, CPUDIV = OSC1_PLL2
#pragma config PWRT = ON, BOR = OFF, BORV = 0
#pragma config WDT = OFF, WDTPS = 32768
#pragma config MCLRE = ON, LPT1OSC = OFF, PBADEN = OFF, CCP2MX = OFF
#pragma config STVREN = OFF, LVP = OFF, XINST = OFF, DEBUG = OFF
#pragma config CP0 = ON, CP1 = ON, CP2 = ON
#pragma config CPB = ON, CPD = ON
#pragma config WRT0 = ON, WRT1 = ON, WRT2 = ON
#pragma config WRTB = ON, WRTC = ON, WRTD = ON
#pragma config EBTR0 = ON, EBTR1= ON, EBTR2 = ON
#pragma config EBTRB = ON
#define DA Write RC0
    //constants
    float a1 = 1.0;
    float b = 3.0;
    float k0 = -0.;
    float k2 = 4.5; // 1.2;
    float k1 = 5.0; //5.0;
    float TS = 0.01;
    float t1 = 285.;
void main(void)
{
    //initial conditions
    float x1s = .0;
    float y1s = .0;
    float x1 = 0.;
    float y1 = 0.;
    float t0 = .0;
    float xs, ys, x, y, C2, B2, Ts1 ;//, A2, B2, C2;
    TRISB = 0x00;
    TRISD = 0x00;
    while(1)
{
    xs = x1s + Ts*(a1-(x1s*x1s)*y1s-(b+1.0)*x1s );
    ys = y1s + Ts*(-(x1s*x1s)*y1s-(b*x1s));
    y = y1 + Ts*(-(x1*x1)*y1-(b*x1));
    Ts1 = t0 + Ts;
    C2= (k2*(Ts1-t1))*(k2*(Ts1-t1))*(k2*(Ts1-t1))*(k2*(Ts1-t1))/1.;
    B2= k1/(1.+(k2*(Ts1-t1))*(k2*(Ts1-t1))/2.);//+C2);
    x = x1 + Ts*B2 + Ts*(( a1-(x1*x1)*y1-(b+1.0)*x1 )+ k0*(x1-x1s)) ;
    //PORTB = (B2+3.)*17.5;
    PORTB = (xs+3.)*20;    //2.3 ;
    PORTD = (x+3.)*20;
    x1s = xs;
    y1s = ys;
    x1 = x;
    y1 = y;
    t0 = Ts1;
}
}
```

Fig. 7. Program code in mikroC used to implement the pulse-like self-sustained or Brusselator oscillator

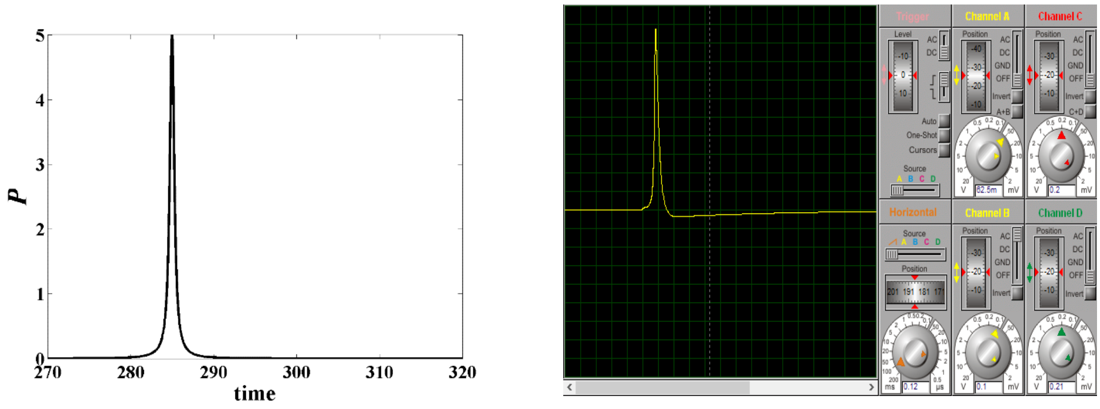

(a) (b)

Fig. 8. The shape of the perturbation is obtained numerically (a) and generated by the microcontroller (b).

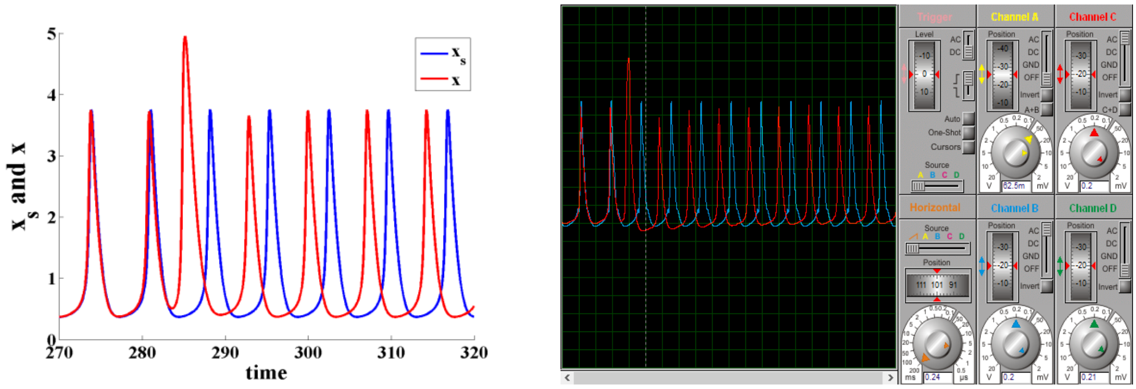

(a) (b)

Fig. 9. The reference oscillator (in blue) and the perturbed oscillator (in red) are generated by the numerical simulation (a) and the microcontroller (b).

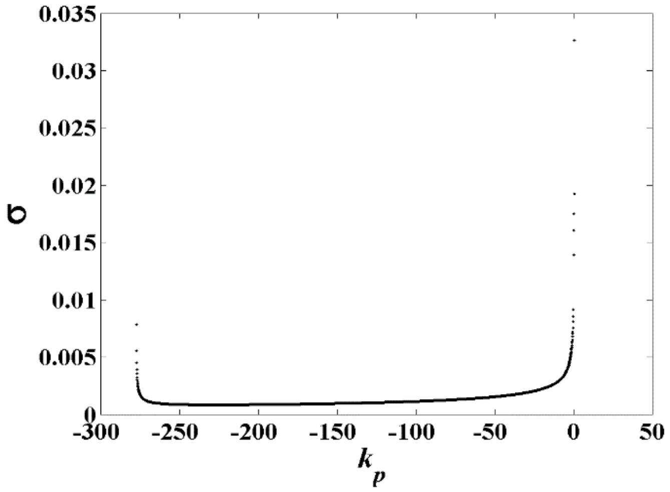

Fig. 10. Normalized average synchronization σ in the case of a Brusselator oscillator subjected to a pulse-like perturbation.

Values of k_p	Temporal trace
-15 for numerical and -5 for microcontroller	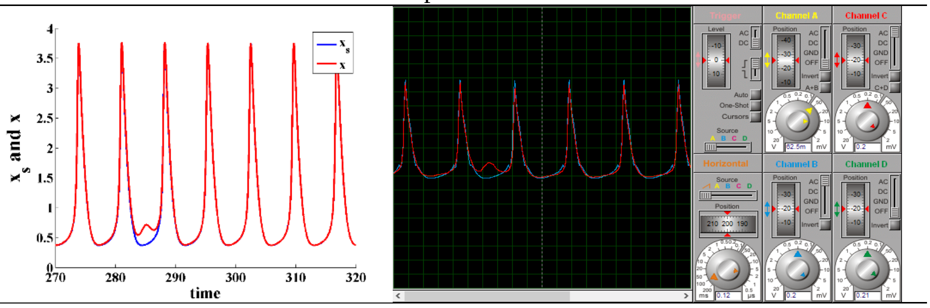
-150	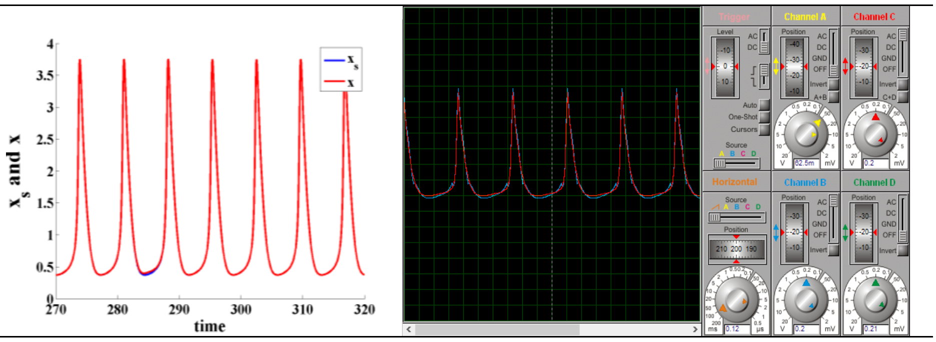

Fig. 11. Two cases present the effectiveness of the control in numerical simulation and in microcontroller-based simulation.

4. Conclusion

The control of pulse-like self-sustained oscillators subjected to perturbations using analog circuits and microcontrollers has been considered in this paper. This has been done using the linear proportional control. The implementation of the control has been done using three simulation methods: numerical simulation, analog electronic simulation and microcontroller-based simulation. The synchronization intervals have been found from the numerical simulation by plotting the synchronization time. It has been found that the control degrades as the linear proportional control increases and is good for small values. The implementation in the microcontroller uses the software mikroC PRO for PIC. The results from the microcontroller simulation have demonstrated that it is an efficient way to produce and synchronize self-sustained electric signals that have been generated from analog electronic circuits. The synchronization intervals have been determined from the simulation based on a microcontroller, and the results obtained are interesting and comparable and indicate the interest in using embedded technologies to control the pulse-like oscillator dynamics using microcontrollers. Our next investigation will focus on the experimental implementation of the control strategies using a microcontroller and the extension of the microcontroller control scheme to other dynamical systems.

Acknowledgments: The authors are grateful to the reviewers for the comments they provided, thus making the work better.

Author Contribution: All authors contributed equally to the main contributor to this paper. All authors read and approved the final paper.

Conflicts of Interest: The authors declare no conflict of interest.

Funding: This research received no external funding.

Conflicts of Interest: The authors declare no conflict of interest in preparing this article.

References

[1] E. de Pinto Sandro, R. Lopez Sergio and L. Viana Ricardo, "Collective behavior in a chain of Van der Pol oscillators with power-law coupling," *Physica A: Statistical Mechanics and its Applications*, vol. 303, no. 3-4, pp. 339-356, 2002, https://doi.org/10.1016/S0378-4371(01)00549-0.

[2] B. Ramakrishnan, A. Durdu, K. Rajagopal, and A. Akgul, "Infinite attractors in a chaotic circuit with exponential memristor and Josephson junction resonator," *AEU–International Journal of Electronics and Communications*, vol. 123, p. 153319, 2020, https://doi.org/10.1016/j.aeue.2020.153319.

[3] R. Rand and P. Holmes, "Bifurcation of periodic motions in two coupled Van der Pol oscillators," *International Journal of Non-Linear Mechanics*, vol. 15, no. 4-5, pp. 387-399, 1980, https://doi.org/10.1016/0020-7462(80)90024-4.

[4] J. Murray, *Mathematical biology*. New York: Springer, 2002, https://doi.org/10.1007/b98868.

[5] J. Kozlowski, U. Parlitz and W. Lauterborn, "Bifurcation analysis of two coupled periodically driven Duffing oscillators," *Physical Review E*, vol. 51, no. 3, p. 1861, 1995. https://doi.org/10.1103/PhysRevE.51.1861.

[6] H. Simo, "Etude théorique et expérimentale de la dynamique des oscillateurs pulsés et applications aux systèmes électromécaniques," *Doctorat/PhD thesis, University of Yaounde 1: Yaoundé (Cameroon)*, 2014, http://www.lamsebp.org/PDF/ABSTRACT_SIMO.pdf.

[7] A. Destexhe and P. Gaspard, "Bursting oscillations from a homoclinic tangency in a time delay system," *Physics Letters A*, vol. 173, no. 4-5, pp. 386-391, 1993, https://doi.org/10.1016/0375-9601(93)90256-Y.

[8] E. M. Izhikevich, "Neural excitability, spiking and bursting," *International Journal of Bifurcation and Chaos*, vol. 10, no. 6, pp. 1171-12660, 2000, https://doi.org/10.1142/S0218127400000840.

[9] Q. S. Bi, "The mechanism of bursting phenomena in Belousov-Zhabotinsky (BZ) chemical reaction with multiple time scales," *Science China Technological Sciences*, vol. 53, pp. 748-760, 2010, https://doi.org/10.1007/s11431-010-0082-8.

[10] U. Simo Domguia, "Theoretical and experimental study of electromechanical systems powered by bio/chemo-inspired oscillators," *Doctorat/Ph.D. thesis, University of Yaounde 1: Yaoundé (Cameroon)*, 2019.

[11] M. Tlidi, Y. Gandica, G. Sonnino, E. Averlant and K. Panajotov, "Self-replicating spots in the Brusselator model and extreme events in the one-dimensional case with delay," *Entropy*, vol. 18, no. 3, p. 64, 2016, https://doi.org/10.3390/e18030064.

[12] L. W. Luyben, *Chemical Reactor Design and Control*. Wiley & Sons, New York, USA: 2007, https://books.google.co.id/books?id=P-zvB8z3djYC.

[13] O. Levenspiel, *Chemical Reaction Engineering*. Wiley & Sons, New York, USA: 1999, https://books.google.co.id/books?id=vw48EAAAQBAJ.

[14] R. Thepi Siewe, "Microcontroller and analog study of the synchronization of coupled Van der Pol oscillators," *Doctorat/Ph.D. thesis, University of Yaounde 1: Yaoundé (Cameroon)*, 2020.

[15] F. Wang, L. Zhang, X. Feng and H. Guo, "An Adaptive Control Strategy for Virtual Synchronous Generator," *Transactions on Industry Applications*, vol. 54, no. 5, pp. 5124-5133, 2018, https://doi.org/10.1109/TIA.2018.2859384.

[16] W. Bai, T. Li and S. Tong, "NN Reinforcement Learning Adaptive Control for a Class of Nonstrict-Feedback Discrete-Time Systems," *IEEE Transactions on Cybernetics*, vol. 50, no. 11, pp. 4573-4584, 2020, https://doi.org/10.1109/TCYB.2020.2963849.

[17] L. Liu, T. Gao, Y. J. Liu, S. Tong, C. L. Philip Chen and L. Ma, "Time-varying IBLFs-based adaptive control of uncertain nonlinear systems with full state constraints," *Automatica*, vol. 129, p. 109595, 2021, https://doi.org/10.1016/j.automatica.2021.109595.

[18] R. Chiu R, Mora-Gonzalez and Lopez-Mancilla, "Implementation of a Chaotic Oscillator into a Simple Microcontroller," *IERI Procedia*, vol. 4, pp. 247-252, 2013, https://doi.org/10.1016/j.ieri.2013.11.035.

[19] H. Hamiche, S. Guermah, R. Saddaoui, K. Hannoun, M. Laghrouche, and S. Djennoune, "Analysis and implementation of a novel robust transmission scheme for private digital communications using Arduino Uno board," *Nonlinear Dyn.*, vol. 81, no. 4, pp. 1921-1932, 2015, https://doi.org/10.1007/s11071-015-2116-z.

[20] A. P. Fournaris and N. Sklavos, "Secure embedded system hardware design - A flexible security and trust enhanced approach," *Comput. Elect. Eng.*, vol. 40, no. 1, pp. 121–133, 2014. https://doi.org/10.1016/j.compeleceng.2013.11.011.

[21] A. A. Elbaset, H. Ali, M. Abd-El Sattar and M. Khaled, "Implementation of a modified perturb and observe maximum power point tracking algorithm for photovoltaic system using an embedded microcontroller," *IET Renew Power Gen*, vol. 10, no. 4, pp. 551–560, 2016, https://doi.org/10.1049/iet-rpg.2015.0309.

[22] M. A. Murillo-Escobar, C. Cruz-Hernández, F. Abundiz-Pérez and R. M. López-Gutiérrez, "Implementation of an improved chaotic encryption algorithm for real-time embedded systems by using a 32-bit microcontroller," *Microprocess. Microsyst.*, vol. 45, pp. 297–309, 2016. https://doi.org/10.1016/j.micpro.2016.06.004

[23] S. Kaçar, "Analog circuit and microcontroller based RNG application of a new easy realizable 4D chaotic system," *Optik*, vol. 127, no. 20, pp. 9551-9561, 2016, https://doi.org/10.1016/j.ijleo.2016.07.044.

[24] J. Chandramohan, R. Nagarajan, K. Satheeshkumar, N. Ajithkumar, P. A. Gopinath and S. Ranjithkumar, "Intelligent smart home automation and security system using Arduino and Wi-fi," *Int. J. Eng. And Comp. Sci.*, vol. 6, no. 3, pp. 20694–20698, 2017.

[25] Y. Raghavender Rao, "Automatic smart parking system using Internet of Things (IoT)," *Int. J. Eng. Tech. Sci. Res.*, vol. 4, no. 5, pp. 225–228, 2017, http://www.ijetsr.com/images/short_pdf/1495021347_nitttr888_ijetsr.pdf.

[26] M. Z. De la Hoz, L. Acho and Y. Vidal, "An experimental realization of a chaos-based secure communication using Arduino microcontrollers," *The Scientif. World J.*, vol. 2015, 2015. https://doi.org/10.1155/2015/123080.